Electrochemical deposition of bimetallic sulfides on novel BDD electrode for bifunctional alkaline seawater electrolysis

Mingxu LI [1, 2], Genjie CHU [1, 2], Jiyun GAO [1, 3], Xiaolei YE [1, 2*], Ming HOU [1, 2], Shenghui GUO [1, 2], Yunchuan LI [1, 2], Ziqi ZHOU [1, 2], Li YANG [1, 2*], Pascal BRIOIS[4]

1. Faculty of Metallurgical and Energy Engineering, Kunming University of Science and Technology, Kunming 650093, China
2. State Key Laboratory of Complex Nonferrous Metal Resources Clean Utilization; Faculty of Metallurgical and Energy Engineering, Kunming University of Science and Technology, Kunming 650093, China
3. School of Chemistry and Environment, Yunnan Minzu University, Kunming 650093, China
4. FEMTO-ST Institute (UMR CNRS 6174), UBFC/UTBM. Site de Montbéliard, F-90010 Belfort-France

Corresponding author: Xiaolei YE (Stoneye2@163.com); LI Yang (yanglikmust@163.com)

Abstract

Seawater electrolysis is an ideal technology for obtaining clean energy—green hydrogen. Developing efficient bifunctional catalysts is critical for direct seawater electrolysis to produce hydrogen. Currently, seawater electrolysis electrodes in the form of metal substrates loaded with active catalysts are widely used. However, the challenge of metal corrosion cannot be ignored. In this work, the boron-doped diamond (BDD) with excellent corrosion resistance as a substrate to load active catalysts for seawater electrolysis were explored. The step-by-step electrodeposition method was used for FeCoS/Ni/BDD electrode preparation, which solved the problem that the FeCoS active layer was difficult to adhere to the BDD substrate. The as prepared FeCoS/Ni/BDD electrode exhibits interesting bifunctional catalytic properties with the OER and HER overpotential of 425 mV and 360 mV in alkaline-simulated seawater (containing 1 M KOH and 3.5 wt. %NaCl) at a current density of 100 mA cm^{-2}. At the same time, by adjusting the KOH concentration in the alkaline-simulated seawater (increased to 3 M), the OER and HER overpotentials of the electrode dropped sharply to 383 mV and 300 mV, respectively. This work provides a new idea for the use of BDD substrates in the design of alkaline seawater electrolysis electrodes with excellent corrosion resistance.

Keywords: Boron doped diamond, seawater electrolysis, bifunctional catalytic, bimetallic sulfides, corrosion resistance

1. Introduction

As fossil energy becomes increasingly scarce and environmental pollution becomes more prominent, the development of renewable clean energy has become urgent [1,2]. In many renewable energy sources, hydrogen energy is regarded as an ideal alternative to traditional fossil fuels due to its high energy density, excellent calorific value and high environmental friendliness [3-5]. Currently, hydrogen energy is mainly produced from fossil fuels, industrial by-products, methanol reforming and water electrolysis [6,7]. Hydrogen production from electrolyzed seawater is the most desirable option for preparing hydrogen because it is clean and has zero carbon emissions[8-10]. Development of hydrogen production from electrolyzed water is limited by overpotential energy loss[11-13]. Hydrogen production through electrolysis of water, where catalysts play a key role in economic viability and environmental sustainability, is demonstrated. Platinum electrodes are widely used in three-electrode devices for electrochemical analysis because of their excellent electrochemical inertness, electrical conductivity and mechanical stability [14], but it still faces the problems of high potential and high price. The corrosion resistance of transition metal sulfides (TMS) is significantly enhanced in both acidic and alkaline environments [15-18]. The electronic structure of sulfides was effectively modulated by the introduction of defects, vacancies and morphology modulation by Hui Su et al. which resulted in the lowering of the OER energy barriers and the enhancement of the electrochemical properties [17,19,20]. Nickel foam (NF) was treated with Al-doped Ni_3S_2 to obtain Al-Ni_3S_2/NF composites by Wei Liu et al. The test results indicated that the low overpotentials of HER and OER were determined to be 86 mV and 223 mV at a current density of 10 mA/cm^2 in 1 M KOH solution, respectively [21]. Nickel foam metal substrates have significant advantages such as high electrical conductivity, large specific surface area, high mechanical strength and easy processing. However, under industrial grade electrolyzed water conditions, nickel foam or copper foam metal substrates face a number of corrosion resistance issues. This means that under extreme conditions, substrates with better corrosion resistance and a wider range of applications need to be found.

The corrosion resistance of BDD electrodes in complex environments is mainly due to their unique electrochemical properties and potential for application in specific environments [16,22]. BDD electrodes show excellent corrosion resistance and catalytic activity in wastewater treatment, effectively treating difficult-to-degrade industrial wastewater and enhancing its biochemistry[23,24]. In certain gas detection applications, the BDD is able to be used as a sensor in corrosive gas environments, such as chlorine and sulfur dioxide[22,25-27]. Electrodes made of BDD are commonly used for the detection of heavy metal ions such as lead and mercury in water bodies[22,28]. Due to the high corrosion resistance of the BDD electrode, it can avoid a series of energy consumption problems caused by corrosion problems of the metal substrate compared to the traditional metal electrode. Therefore, in this paper, we attach cobalt-iron sulfide to the BDD electrode, thus circumventing some related problems. And there is a lack of research on current hotspots such as seawater electrolysis. Therefore, it is necessary to expand more electrochemical applications of BDD electrodes and to study the feasibility and practicality of their application.

In this paper, we report a two-step process for fabricating CoFeS/Ni/BDD electrodes, involving electroplating a nickel layer onto BDD electrodes and subsequently depositing cobalt-iron sulfides electrochemically. The structure and morphology of the crystals were characterized by XRD and SEM, and the electrochemical properties of the electrodes were tested by means of LSV, CV and EIS. Increasing the concentration of KOH reduces the overpotential for both hydrogen and oxygen evolution reactions, offering a new approach to lowering the evolution potentials.

2. Experimental

2.1 Materials

Boron-doped diamond (BDD, 10 mm × 10 mm, single side) was purchased from New Peak Technology Co. Nickel metal plate (Ni, 25 mm × 25 mm × 1.5 mm) was purchased from Seiko Metal Materials Co. Ammonium chloride (NH_4Cl), nickel chloride ($NiCl_2 \cdot 6H_2O$), ferric chloride hexahydrate ($FeCl_3 \cdot 6H_2O$), ammonia (NH_3), potassium hydroxide (KOH), sodium chloride (NaCl), thiourea (CH_4N_2S), potassium chloride (KCl), anhydrous ethanol (C_2H_5OH) were purchased from Tianjin Zhiyuan Chemical Reagent Co.

2.2 Preparation of Ni/BDD electrode

Before electroplating, the boron-doped diamond (BDD) electrode, and the BDD surface were first degreased to eliminate the effect of impurities on the electroplating process. This step consisted of immersing the BDD surface in a solution of 1 M HCl and 1 M NaOH and ultrasonic treatment using an ultrasonic cleaner for 30 min, followed by rinsing the surface with anhydrous ethanol and deionized water for five times each to ensure that the surface was clean and free of nickel powder, and then drying the electrodes in an oven at 50 °C. Then, electroplating was used to deposit nickel metal on the treated BDD surface. The process first involved configuring 100 mL of a mixed solution (0.1 M $NiCl_2$ + 2 M NH_4Cl). In the electroplating process, a DC power supply was used to control a constant current of 0.1 A. The BDD electrode was used as the cathode and the nickel plate as the anode. Next, BDD electrodes with dimensions of 5 mm × 10 mm were immersed in an electrolyte at a temperature of 20°C and electroplated for 30 min to successfully prepare Ni/BDD electrodes.

2.3 Preparation of CoFeS/Ni/BDD electrode

Cobalt-iron sulfides were electrochemically deposited onto prepared Ni/BDD electrodes. The electrodeposition experiments were carried out in a three-electrode system with an electrolyte consisting of a mixture of $NiCl_2$, $FeCl_3$ and thiourea. Ni/BDD electrodes were used as working electrodes, Ag/AgCl electrodes as reference electrodes, and carbon rods as counter electrodes. The concentrations of cobalt and iron in the electrolyte directly determine the content of cobalt and iron in the deposited layer, which in turn affects the electrocatalytic performance. Therefore, CoFeS/Ni/BDD electrodes were synchronously prepared in three sets of electrolytes with different cobalt and iron concentrations while keeping other conditions constant, where the concentration ratio of $NiCl_2$ to $FeCl_3$ was set at 1-3 (7.5 mM: 7.5 mM-22.5 mM: 7.5 mM). The number of electrodeposition cycles is directly related to the amount of cobalt, iron and sulfur deposited onto the Ni electrode. This remains a key factor influencing the electrocatalytic performance of the electrode. For this purpose, four CoFeS/Ni/BDD electrodes were prepared by cyclic voltammetry with a set scan rate of 5 mVs^{-1} and a scan range of -0.6-0.2 V. Each electrode underwent a different number of electrodeposition cycles (5-20 turns). Finally, the appropriate cobalt-iron concentration and number of electrodeposition turns were selected based on the catalytic performance performance of these electrodes in 1 M KOH solution.

2.4 Material characterization

The BDD electrode-related information was characterized on a Bruker D8-Advance x-ray diffractometer (Cu Kα, λ = 1.5406 Å) with a scanning speed of 3 degrees per minute and a scanning range of 10° to 100°. The diamond samples and the precursor materials of the diamond-based electrodes were characterized morphologically and microzonally analyzed for their chemical composition using a Quanta 200 scanning electron microscope from FEI, USA. The surface elemental composition as well as the chemical valence states of the samples were resolved using multifunctional scanning imaging photoelectron spectroscopy of PH5000Versaprobe-with A1Ka as the X-ray light source at 50 w and 15 kV.

2.5 Electrochemical measurements

On the three-electrode system of the Shanghai Chenhua CHI760e electrochemical workstation, we conducted electrochemical tests, including cyclic voltammetry (CV), linear scanning voltammetry (LSV), and alternating current impedance (EIS). These tests were used for seawater electrolysis experiments, respectively. In this setup, the three-electrode system had a BDD or BDD-based composite electrode as the working electrode with an electrode area of 10×10 mm^2 and an area of 10×5 mm^2 immersed in the solution. Hg/HgO or Ag/AgCl electrodes served as the reference electrodes, and a carbon rod served as the counter electrode.

3 Results and Discussion

3.1 Synthesis and structural characterization

Fig.1 shows the surface morphology and chemical composition of the electrode samples at different stages throughout the preparation process. Smooth polycrystalline pyramidal structure features can be observed on high quality BDD surfaces. The tightly textured boron-doped diamond films are formed by their intricate arrangement (Fig.1a). As shown in the SEM images of Ni/BDD samples at different magnifications in Figs.1b-c, agglomeration of cauliflower-like particles and uniform distribution of columns can be clearly observed. The grooves between each column are well-defined, which effectively increases the specific surface area and allows more active sites to be exposed. The morphology of CoFeS/Ni/BDD electrode after electrodeposition is depicted in Figs.1d-f. A large amount of lamellar material was observed dispersed on the surface of the columnar structure and embedded in the surface of the cauliflower-like particles. This morphological change is indicated by the attachment of a new substance of iron cobalt sulfide to the electrode surface. Furthermore, the constituent elements of the CoFeS/Ni/BDD electrode surface were analyzed (Figs.1g-h). The results indicate that the nickel particles are completely encapsulated by these uniformly distributed elements. Combined with the analysis of elemental content in Fig.1h, it is evident that the elements Co, Fe, and S were deposited onto the surface of Ni/BDD to form a CoFeS/Ni/BDD electrode. Three Ni diffraction peaks (PDF 04-0850) are shown at 44.51°, 51.84°, and 76.37°, as demonstrated by the XRD spectra of the heat-treated CoFeS/Ni/BDD electrodes in Fig.2. The associated diffraction peaks of Ni-Co-S correspond to the standard card (JSCPDS43-1477), and this was observed simultaneously [29]. However, no obvious peaks of cobalt sulfide were observed, which could be attributed to the small amount deposited during electrodeposition of CoFeS [30,31]. In addition to this, a large number of Ni_3S_2 diffraction peaks (PDF 44-1418) were observed. None of the observed information about iron sulfide was available, so the electrodeposited iron sulfide was assumed to be amorphous, an assumption that is consistent with the results of the previous tests.

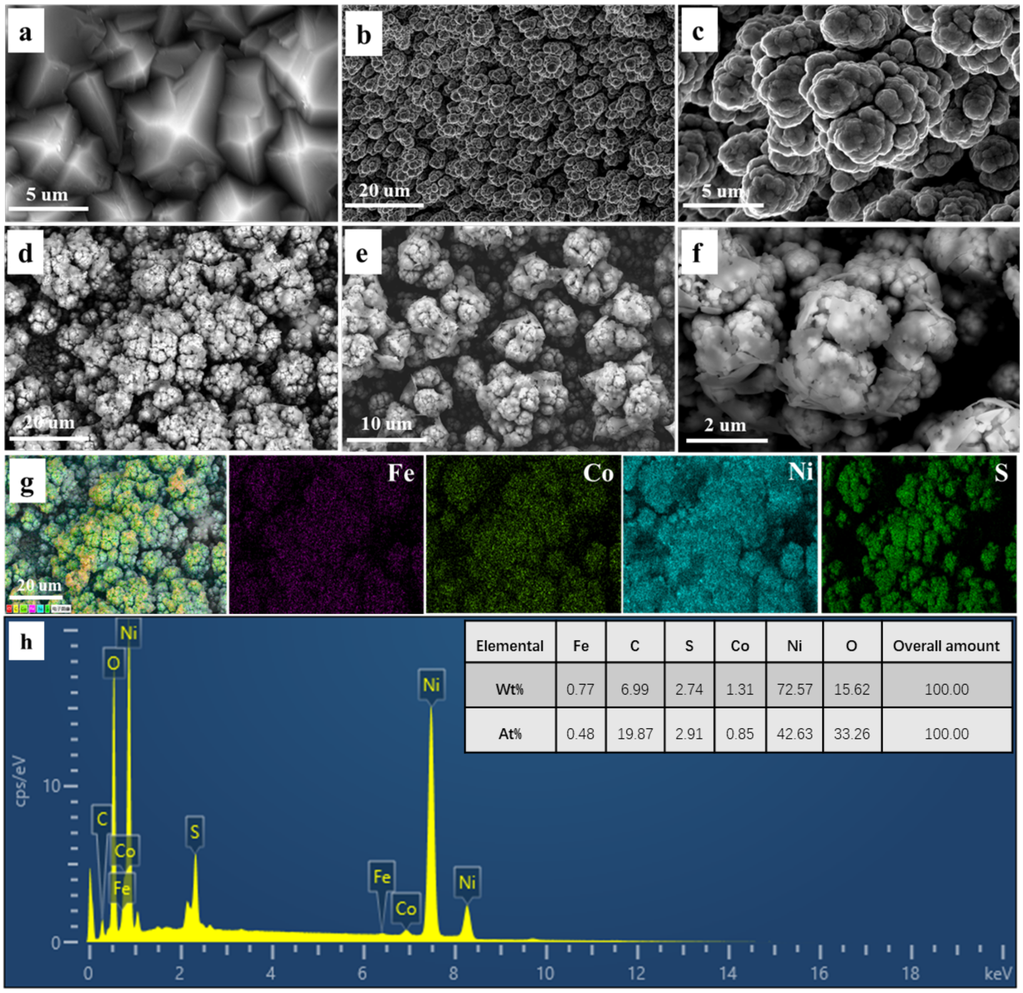

Elemental	Fe	C	S	Co	Ni	O	Overall amount
Wt%	0.77	6.99	2.74	1.31	72.57	15.62	100.00
At%	0.48	19.87	2.91	0.85	42.63	33.26	100.00

Fig.1 (a) SEM images of the original BDD, (b-c) Ni/BDD SEM maps at different magnifications, (d-f) Scanning electron micrographs of CoFeS/Ni/BDD at different magnifications and their (g-h) EDS patterns and analysis of surface element content of CoFeS/Ni/BDD sample

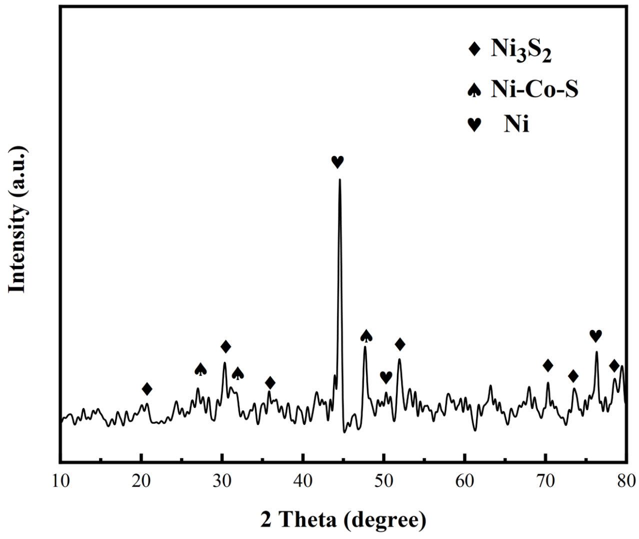

Fig.2 XRD pattern of CoFeS/Ni/BDD electrode.

3.2 Electrochemical Properties

3.2.1 Electrochemical properties of CoFeS/Ni/BDD electrode

The electrode samples indicated in Fig.3 were prepared by electrodeposition in electrolytes with different cobalt and iron concentrations. The hydrogen evolution reaction and oxygen evolution reaction properties of the electrode samples were tested in 1 M KOH solution to explore the optimal deposition parameters for cobalt and iron concentrations.

CoFeS/Ni/BDD electrode materials are prepared by Co-Fe deposition technology. The electrochemical activity of this electrode was evaluated for HER and OER using various concentrations of Co in 1 M KOH solution, and the linear scanning voltammetry (LSV) curves are shown in Figs.3a-b. The HER and OER overpotential line plots for a single CoFeS/Ni/BDD electrode at 100 mA cm^{-2} and 200 mA cm^{-2} current densities are shown in Fig.3c. Fig.3c reveals that the HER and OER overpotentials of the CoFeS/Ni/BDD samples were observed to be minimized when the Co-Fe concentration ratio was 1.5, indicating that the electrocatalytic performance of this group of samples was optimal. CoFeS/Ni/BDD electrodes mentioned later in this chapter were prepared as samples with a Co-Fe concentration ratio of 1.5, unless otherwise noted.

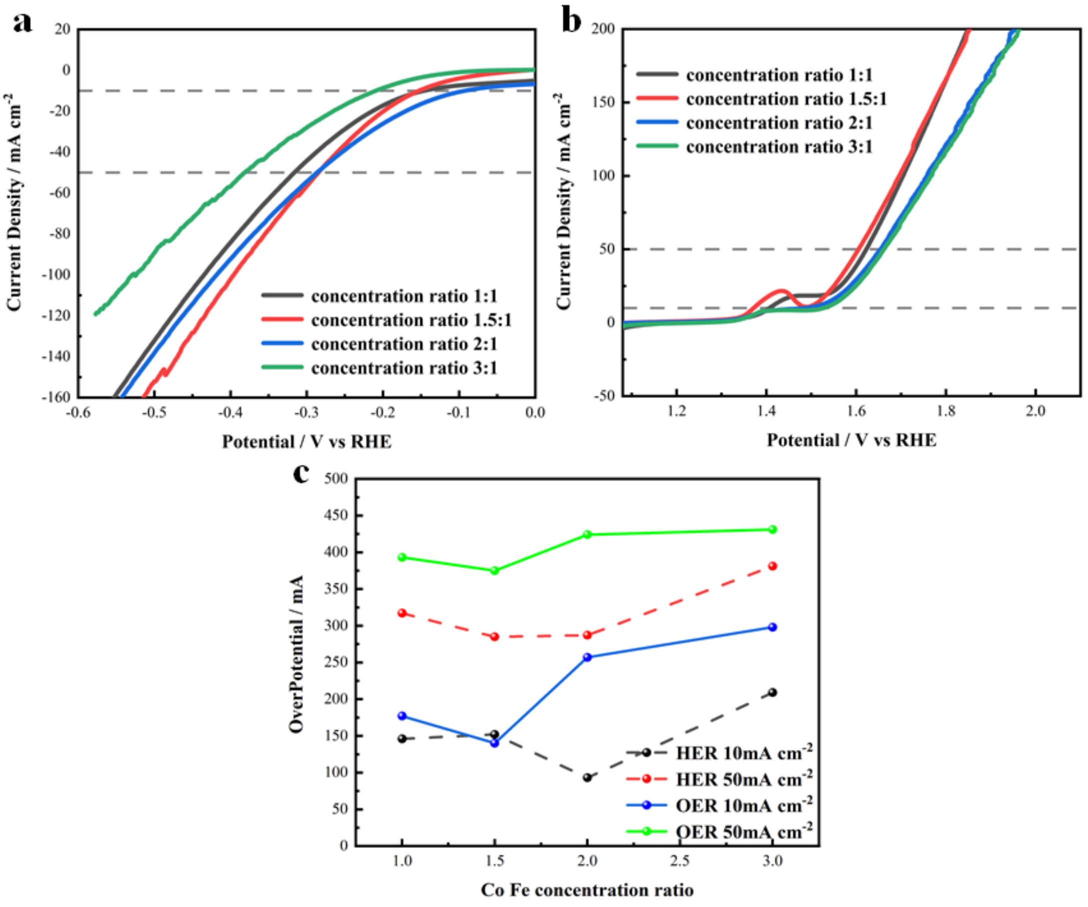

Fig.3 CoFeS/Ni/BDD electrode prepared with different concentration ratios of cobalt and iron(a) HER performance, (b) OER performance and (c) overpotential line graph atcurrent densities of 10mA cm^{-2} and 50mA cm^{-2}.

The HER/OER performance of CoFeS/Ni/BDD electrodes prepared at different number of cycles is depicted in Fig.4. This indicates that different number of cycles has a great influence on the catalytic performance of CoFeS/Ni/BDD electrodes. The electrocatalytic performance of the electrode was worst when only 5 cycles were made, while the catalytic performance gradually improving as the number of cycles increased. However, when the number of cycles reaches 20, the catalytic performance begins to decrease and is roughly equivalent to that achieved at 10 cycles. At the same time, the best HER and OER performance was achieved at 15 cycles (Figs.4 a,b).

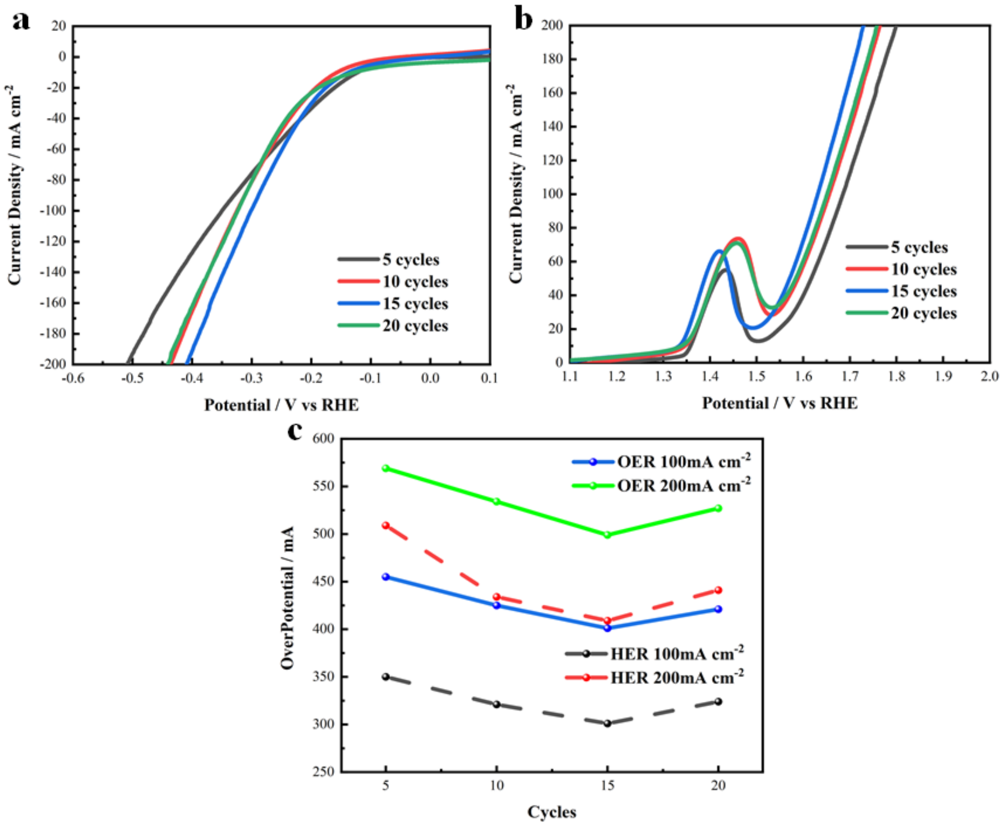

Fig.4 (a) HER performance, (b) OER performance of the CoFeS/Ni/BDD electrode prepared with 5, 10, 15, and 20 electrodeposition cycles in the range of -0.6~0.2V at a scan speed of 5mV/s. and (c) overpotential line graph at 100mA cm^{-2} and 200mA cm^{-2} current densities

As shown in Fig.4c, combined with the analysis of overpotential line graphs of CoFeS/Ni/BDD electrode at 100 mA cm^{-2} and 200 mA cm^{-2} current densities. The HER overpotential values are 301 mA and 409 mA when the number of electrodeposition cycle turns is 15. The overpotential values are lower than 350 mA and 509 mA for 5 turns, 321 mA and 434 mA for 10 turns, and 324 mA and 441 mA for 20 turns. Similarly, the OER was lowest at 15 turns of cycling, with overpotential values of 401 mA and 499 mA, both of which are smaller than the overpotential values at 5 (455 mA, 569 mA), 10 (425 mA, 534 mA), and 20 (421 mA, 537 mA) turns of cycling.

In summary, the optimal process for the preparation of CoFeS/Ni/BDD electrodes by cyclic voltammetry electrodeposition was finally determined as 15 cycles at a sweep rate of 5 mV/s in the range of -0.6~0.2 V.

3.2.2 HER catalytic performance of CoFeS/Ni/BDD

To assess the hydrogen evolution performance of the CoFeS/Ni/BDD electrode, pristine BDD, Ni/BDD, and CoFeS/Ni/BDD electrodes were evaluated in a 1 M KOH standard solution and an alkaline simulated seawater solution containing 3.5% NaCl and 1 mol/L KOH. Furthermore, to emphasize the influence of KOH concentration on the electrocatalytic effect, a control set of alkaline solution containing 3.5% NaCl and 3 mol/L KOH was included. Nitrogen was passed into the solution for 20 minutes prior to testing to eliminate interference from dissolved oxygen. Fig.5a presents the linear scanning voltammetry (LSV) curves of the pristine BDD, Ni/BDD, and CoFeS/Ni/BDD tri-electrodes in a 1 M KOH standard solution, as well as the LSV curves of the CoFeS/Ni/BDD electrode in alkaline simulated seawater (Figure CoFeS/Ni/BDD-sea) at a sweep rate of 5 mV/s. In 1 M KOH, the pristine BDD electrode exhibited negligible HER activity, and the Ni/BDD electrode had an overpotential of 345 mV. The CoFeS/Ni/BDD electrode, however, showed an overpotential of 325 mV, indicating a 5.7% reduction, which suggests that partial substitution of the Ni surface with NiCo, Ni_3S_2, etc., enhances HER activity, particularly at high current densities. In alkaline simulated seawater, the overpotential increased to 360mV due to the reduction in HER activity by NaCl. When the KOH concentration was increased to 3M, the overpotential was reduced to 300mV, which is lower than that of the 1M KOH standard solution. This change suggests that increasing the KOH concentration helps to improve the catalytic performance. The HER Tafel slope, as in Fig.5b, is then converted from the LSV curve in Fig.5a. The CoFeS/Ni/BDD electrode exhibits a slope of 113.15 mV/dec in 1 M KOH, which increases to 130.81 mV/dec in alkaline simulated seawater. The Ni/BDD electrode has a higher slope of 165.92 mV/dec compared to that of the CoFeS/Ni/BDD electrode. Upon increasing the KOH concentration, the slope decreases to 108.88 mV/dec. By comparing the Tafel slopes of the electrodes, the CoFeS/Ni/BDD electrode is seen to significantly enhance the HER kinetics, an effect hypothesized to arise from the strong catalytic capabilities of the novel materials, such as nickel-cobalt alloys and nickel-iron sulfides, along with the increased specific surface area resulting from morphological changes, collectively improving the electrode's catalytic performance.

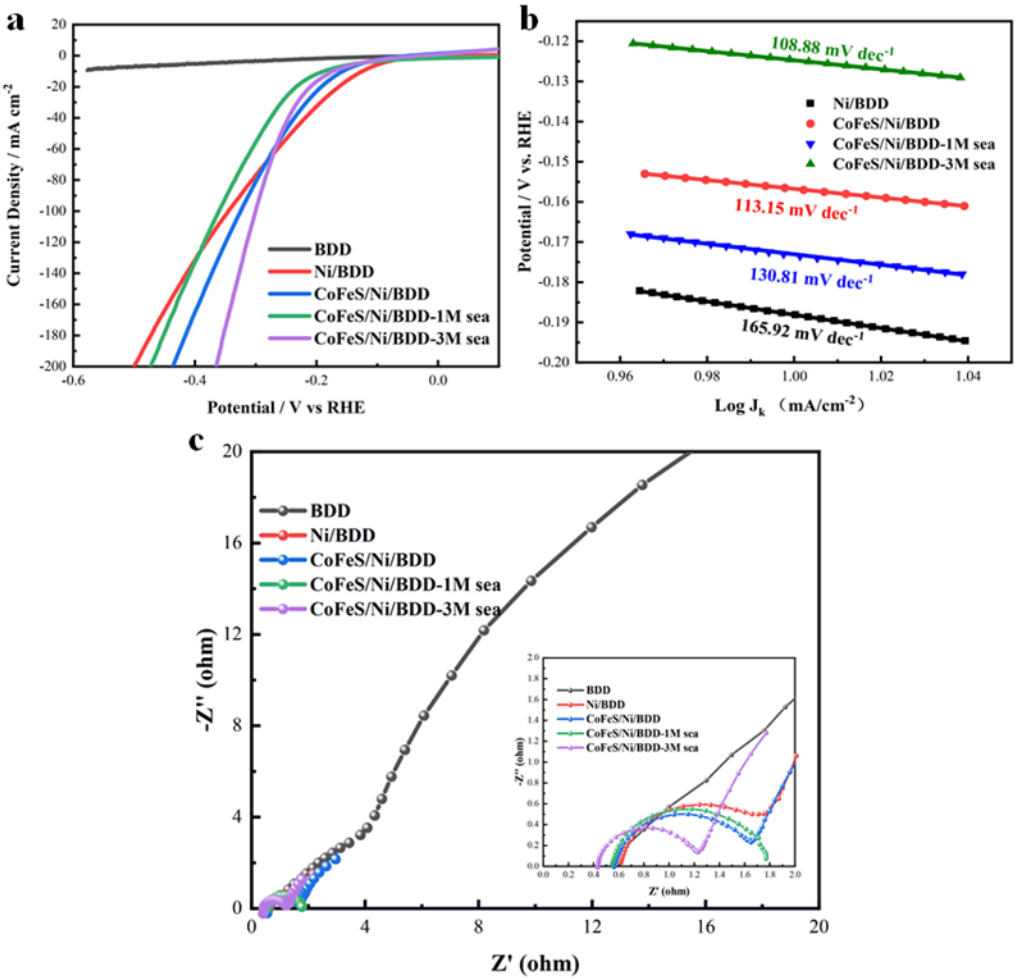

Fig.5(a) LSV inverse scan curve of each electrode of BDD, Ni/BDD, and CoFeS/Ni/BDD scanned in 1 M KOH solution or alkaline simulated seawater (1 M/3 M) at a scan rate of 5 mV/s. (b) Current Tafel curve when the density is 10 mA cm^{-2}. (c) EIS curve relative to Hg/HgO when the potential is -1.1 V

As in Fig.5c, The charge transfer kinetics at the electrodes as well as at the electrolyte interface were investigated in relation to the electrochemical impedance in the frequency range of -1.1 Vs Hg/HgO, 10 kHz to 0.01 kHz. All three electrodes, BDD, Ni/BDD and CoFeS/Ni/BDD, were placed in 1 M KOH solution for testing. The data obtained was plotted as a Nyquist semicircle by the software, and the magnitude of the charge transfer resistance (Rct) during the reaction was determined by comparing the radius of its semicircle.

The results demonstrate that CoFeS/Ni/BDD has the smallest Nyquist radius indicating small Rct and fast charge transfer during the oxygen evolution reaction.The

Nyquist semicircle in the 3M KOH simulated seawater solution was the smallest, indicating the lowest Rct and the fastest charge transfer rate. This is due to the fact that an increase in the KOH concentration increases the ions in the solution, leading to a lower resistance.

3.2.3 OER catalytic properties of CoFeS/Ni/BDD

The electrodes at each preparation stage were analyzed for OER catalytic activity in 1 M KOH solution and alkaline simulated seawater. Prior to each test, the solution was subjected to oxygenation for approximately 20 minutes to ensure that sufficient oxygen was held to ensure the accuracy of the test. Fig.6a displays LSV curves for pristine BDD, Ni/BDD, and CoFeS/Ni/BDD electrodes in 1 M KOH and CoFeS/Ni/BDD in alkaline seawater (CoFeS/Ni/BDD-sea) at 5 mV/s. Pristine BDD shows poor oxygen evolution. Ni/BDD, with a cauliflower-like Ni layer, reaches 1.685 V at 100 mA cm^{-2}, indicating a 455 mV overpotential.

The corresponding potentials of CoFeS/Ni/BDD electrodes are 1.631 V and 1.655 V, respectively (the overpotentials are 401 mV and 425 mV) in a 1 M KOH solution with a current density of 100 mA cm^{-2} and in alkaline simulated seawater. CoFeS/Ni preparation significantly improves the OER catalytic effect, especially at high current density. Increasing the KOH concentration significantly reduces the oxygen evolution activation energy, especially in seawater, which helps to inhibit the side reactions.

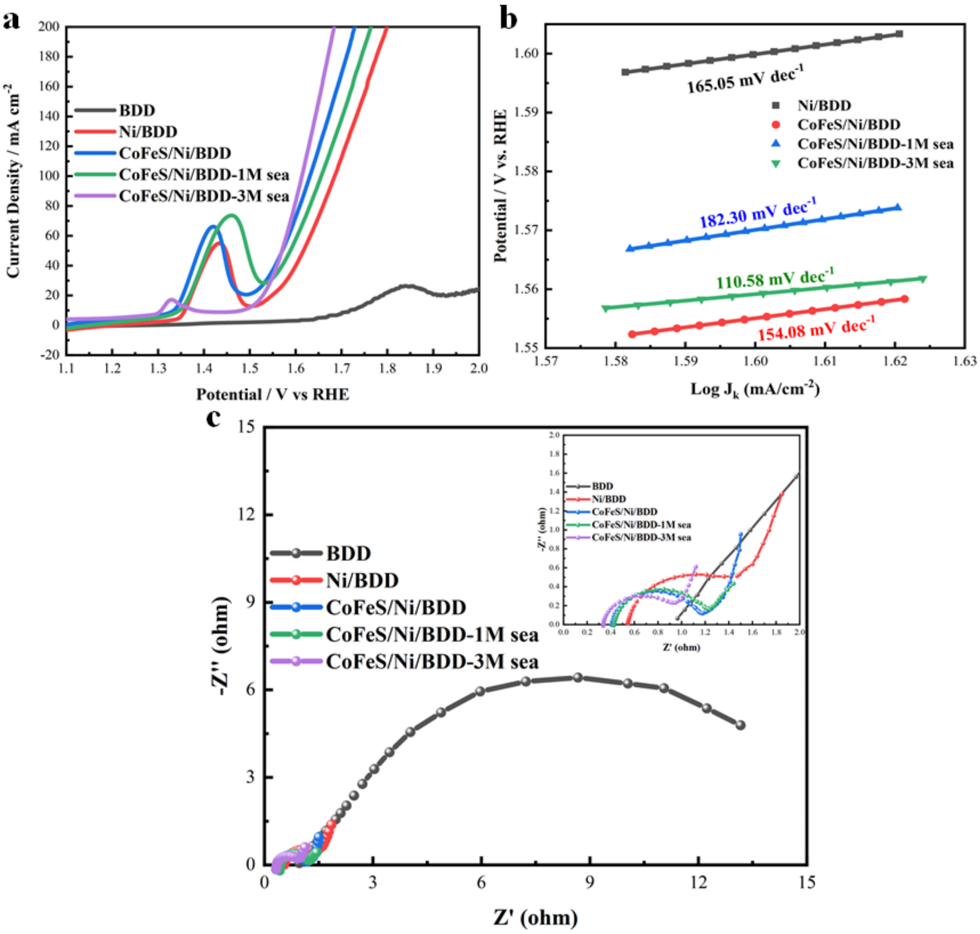

Fig.6(a) LSV inverse scan curve of each electrode of BDD, Ni/BDD, and CoFeS/Ni/BDD scanned in 1 M KOH solution or alkaline simulated seawater (1 M/3 M) at a scan rate of 5 mV/s. (b) Current Tafel curve when the density is 100 mA cm^{-2}. (c) EIS curve relative to Hg/HgO when the potential is 0.6 V.

The Tafel curve for the oxygen evolution reaction is obtained by computational conversion from the LSV curve. As shown in Fig.6b, the Tafel slope value of CoFeS/Ni/BDD electrode in 1 M KOH standard solution was calculated by fitting to be 154.08 mV/dec. The Tafel slope value for this electrode increased to 182.30 mV/dec in alkaline simulated seawater. In contrast, Tafel slope values of only 110.58 mV/dec were observed for CoFeS/Ni/BDD electrodes in alkaline simulated seawater at 3 M KOH. The Tafel slope value of 165.05 mV/dec was observed on the Ni/BDD electrode without electrodeposition treatment and this value is higher than that presented by the electrode modified with cobalt iron sulfide. Observations show that the electrode's kinetic reactivity in the oxygen evolution reaction (OER) is significantly improved by the introduction of cobalt-iron sulfide, and this performance enhancement is attributed to the high electrical conductivity of CoFeS as well as the facilitation of the partial oxidative conversion of the surface catalyst to cobalt-iron oxide. It is concluded that the oxygen evolution reaction process is indeed hindered by side reactions in solution, energy is consumed and the catalytic efficiency of the oxygen evolution reaction is consequently reduced.

The solution charge transfer was studied also by electrochemical impedance (Fig.6c). The frequency range of the test was kept the same as in the hydrogen evolution reaction, and the potential was adjusted to 0.6 Vs Hg/HgO in the oxygen evolution reaction. The results indicate that a seawater simulation solution containing 3 M KOH was observed to exhibit minimal Nyquist semicircles, lower Rct values, and promote more rapid charge transfer during the oxygen evolution reaction. The standard solution with 1 M KOH is the next best, and the results are the same as those of the previous HERs, this suggests that the electrolysis of seawater benefits from the preparation of CoFeS as well as an increase in KOH concentration.

The electrode was cycled at different stages at different scanning speeds from 0.1 V to 0.2 V relative to Hg/HgO in 1 M KOH solution to study the process of electrodeposition of cobalt iron sulfide layer. Under the same conditions, the nickel layer on the electrode underwent periodic scanning to probe the changes in ESCA at different stages. Figs.7a-c shows the pristine BDD, Ni/BDD and CoFeS/Ni/BDD electrode CV curves, respectively. Fig.7d shows the relationship between the current density difference ΔJ and the scanning speed (electric double layer capacitor) for each sample. The Cdl of the CoFeS/Ni/BDD electrode is 3.399×10^{-2} mF/cm^2, which is about 21.93 times higher than that of the pristine BDD electrode of 1.550×10^{-3} mF/cm^2 and 1.53 times higher than that of the Ni/BDD electrode (Cdl 2.226×10^{-2} mF/cm^2).

First, the BDD substrate is electroplated with a layer of nickel, which forms cauliflower-like agglomerates that give the BDD surface a columnar and well-defined shape, thus significantly increasing the specific surface area. Subsequently, nickel cobalt sulfide was prepared by electrodeposition on the surface of the nickel layer, which further increased the specific surface area and thus effectively increased the contact area between the electrolyte and the catalyst.

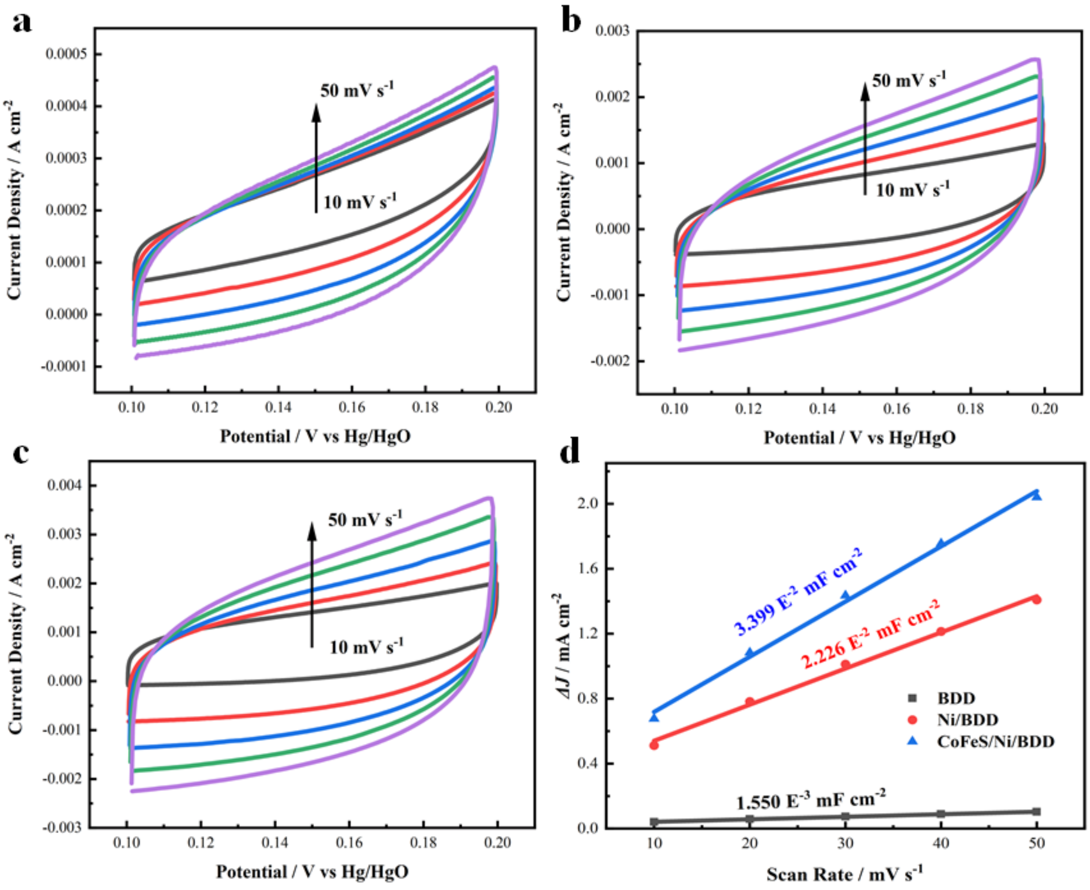

Fig.7(a-c) CV curves of BDD, Ni/BDD and CoFeS/Ni/BDD electrodes at different scanning speeds in the range of 0.1~0.2 V vs. Hg/HgO in 1 M KOH solution, (d) and the current density difference ΔJ versus scanning speed relationship curve between.

3.2.4 Effect of different potassium hydroxide concentrations on the electrocatalytic performance of CoFeS/Ni/BDD of CoFeS/Ni/BDD

During the electrolysis of seawater, some side effects can be headache-inducing. These side reactions compete with the oxygen evolution reaction and significantly impact the efficiency of oxygen generation on the anode. Therefore, enhancing the priority and efficiency of anodic oxygen evolution reactions during seawater electrolysis and investigating effective methods to limit or eliminate competing side reactions have emerged as key areas of current research.

The OER activities of CoFeS/Ni/BDD were all significantly enhanced with increasing KOH concentration (Fig.8b) in the electrocatalytic process. The oxygen evolution overpotential in the electrolyte decreases gradually with increasing KOH concentration from 1 M to 4 M when the current density reaches 200 mA cm^{-2}, with overpotential values of 504 mV, 497 mV, 465 mV, and 447 mV, respectively. When the KOH concentration was increased to 3 M, the overpotential was lower than the side-reaction potential of 480 mV in the alkaline seawater electrolyte. Thus, at higher current densities, side reactions at the electrode can be suppressed by increasing the concentration of potassium hydroxide. Similarly, as shown in Fig.8a, the values of hydrogen evolution overpotential with increasing salinity were 473 mV, 426 mV, 408 mV, and 396 mV. The decrease in overpotential with increasing KOH concentration is due to the fact that the ions supplied in the electrolyte increase the collision frequency of the ions during the passage of the current, which promotes the reaction rate. Fig.8c presents the line graphs of HER and OER overpotentials of CoFeS/Ni/BDD electrodes at 100 mA cm^{-2} and 200 mA cm^{-2} current densities in different KOH concentrations. It can be observed that the evolution of both hydrogen and oxygen improves as the concentration of KOH increases, with the optimal catalytic effect observed in a 4 M KOH solution. The OER/HER tafel curves transformed from the LSV curves in Figs.8a,b are shown in Figs.8d,e. Meanwhile, the Tafel slope values of CoFeS/Ni/BDD electrodes were calculated through linear fitting, revealing a significant correlation with the concentration of KOH in the solution. The HER tafel slope of 139.59 mV/dec at 4M KOH is better than 153.76 mV/dec at 3M and 160.29 mV/dec at 2M and significantly better than 165.03 mV/dec at 1M. The OER Tafel slope is similarly reduced, with a value of 48.77 mV/dec at 4M KOH, which is much lower than the 79.51 mV/dec at 1M KOH. Therefore, the catalytic performance of the CoFeS/Ni/BDD electrode is superior at high potassium hydroxide concentrations, and in special cases, the electrocatalytic effect can be improved by increasing the salt concentration.

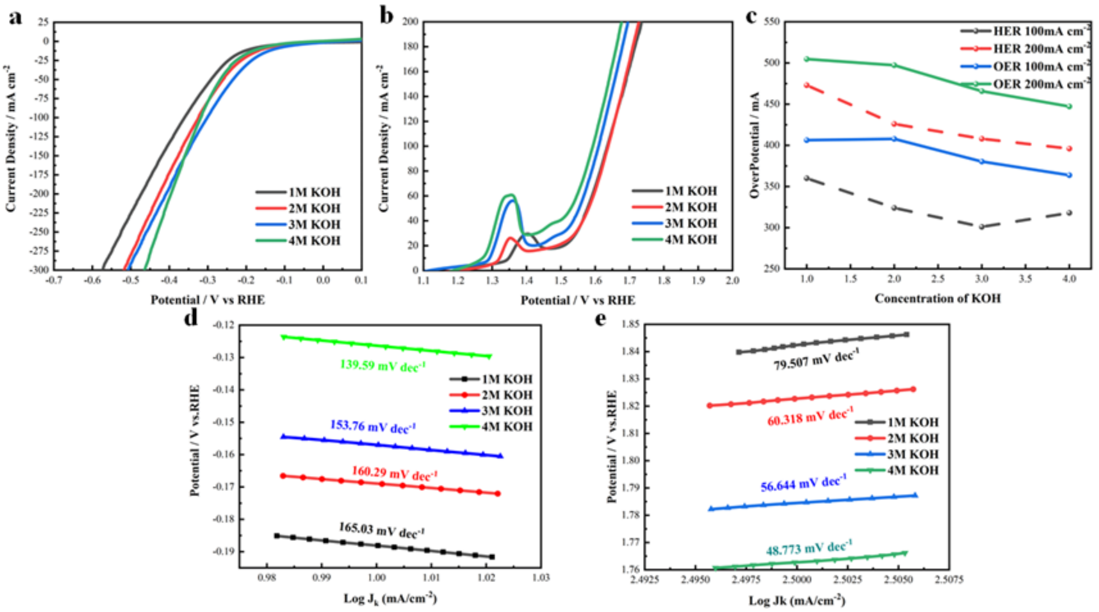

Fig.8 (a) HER. (b) OER. (c) overpotential line diagram of CoFeS/Ni/BDD electrode in 1 M, 2 M, 3 M, 4 M KOH solutions at 100 mA cm^{-2} and 200 mA cm^{-2} current density and (d) Tafel curve of HER at a current density of 10 mA cm^{-2} and (e) Tafel curve of OER at a current density of 200 mA cm^{-2}.

4 Conclusion

In this chapter, a cauliflower-like metallic nickel layer was first plated on the BDD surface. Then, CoFeS/Ni/BDD electrodes with excellent catalytic performance were prepared by electrodepositing cobalt and iron sulfide on the surface of the nickel layer. The effects of the cobalt-iron concentration ratio and the number of electrophoretic cycles on the catalytic performance of the electrodes were investigated, and the optimal process parameters were determined: a cobalt-iron concentration ratio of 1.5, a scanning speed of 5 mV/s, and a cycle number of 15 cycles. It was found that the electrode exhibited low OER and HER overpotentials at a current density of 100 mA cm^{-2} in alkaline simulated seawater. Increasing the KOH concentration could further reduce the overpotentials and directionally promote the oxygen evolution reaction, thus enhancing the efficiency. This study not only extends the application of BDD beyond anodic degradation of organic wastewater, but also shows great potential in the field of seawater electrolysis. At the same time, it opens up new perspectives for the application of BDD.

CRediT authorship contribution statement

Mingxu LI: methodology, formal analysis, investigation, data curation and writing - original draft. Genjie CHU: formal analysis and writing - review & editing. Jiyun GAO: formal analysis. Xiaolei YE: funding acquisition, supervision and writing - review & editing. Ming HOU: formal analysis. Shenghui GUO: funding acquisition, conceptualization. Yunchuan LI: formal analysis and software. Ziqi ZHOU: formal analysis. Li Yang: conceptualization, funding acquisition, supervision and writing - review & editing. Pascal BRIOIS：language review, formal analysis and visualization.

Declaration of Competing Interest

The authors declare that they have no known competing financial interests or personal relationships that could have appeared to influence the work reported in this paper.

Data availability

Data will be made available on request.

Acknowledgement

This research was supported by National Natural Science Foundation of China (52364051, 52374389) and Caiyun Postdoctoral Program in Yunnan Province of China (CG24056E003A, CG24056E014A); The authors (Li Yang, Shenghui Guo) would like to acknowledge Xing Dian talent support program of Yunnan Province.

Reference

1 Prajapati, M. & Shah, M. Geothermal-solar hybrid systems for hydrogen production: A systematic review. *International Journal of Hydrogen Energy* **67**, 842-851, (2024).

2 Dang, V.-H. *et al.* Photocatalytic hydrogen production from seawater splitting: Current status, challenges, strategies and prospective applications. *Chemical Engineering Journal* **484**, 149213 (2024).

3 Du, J., Zhang, X., He, F. & Xie, Y. Modulation of the morphology, composition, and oxidation state of the spinel high-entropy oxides to boost their bifunctional catalytic activity for overall water splitting. *Electrochimica Acta* **461**, 142599 (2023).

4 Santra, S., Das, D., Das, N. S. & Nanda, K. K. An efficient on-board metal-free nanocatalyst for controlled room temperature hydrogen production††Electronic supplementary information (ESI) available. See DOI: 10.1039/c7sc00162b. *Chemical Science* **8**, 2994-3001 (2017).

5 Tarhan, C. & Çil, M. A. A study on hydrogen, the clean energy of the future: Hydrogen storage methods. *Journal of Energy Storage* **40**, 102676 (2021).

6 Jianlin, L., Zhonghao, L., Danxi, L. & Suliang, M. J. D. E. R. Overview of development status of green hydrogen production and application technology under targets of carbon peak and carbon neutrality. **6**, 25-33 (2021).

7 Xu, S. & Yu, B. J. J. o. B. I. o. T. Current development and prospect of hydrogen energy technology in China. **23**, 1-12 (2021).

8 Sun, H. *et al.* Electrochemical water splitting: Bridging the gaps between fundamental research and industrial applications. **6**, e12441 (2023).

9 Liu, Q. *et al.* F-doped self-supporting carbon electrode to improve carbon–water reaction assisted electrolysis of water for hydrogen production. **375**, 132512 (2024).

10 Li, W., Sun, Z., Ye, X. & He, Y. J. I. J. o. H. E. Ultra-thin PPS mesh-based PSF-ZrO2 composite diaphragm for efficient electrolysis of water for hydrogen production. **81**, 918-926 (2024).

11 ZHANG, W.-y. *et al.* Research and perspectives on electrocatalytic water splitting and large current density oxygen evolution reaction. **45**, 1057-1070 (2023).

12 Xie, W.-F. & Shao, M.-F. J. J. o. E. Alkaline water electrolysis for efficient hydrogen production. **28**, 4 (2022).

13 Zhang, Y., Zhang, B. & Sun, J. J. J. o. P. U. Progress in hydrogen production by water electrolysis and its electrocatalysts. **35**, 19 (2022).

14 Wei, R., Fang, M., Dong, G. & Ho, J. C. Is platinum a suitable counter electrode material for electrochemical hydrogen evolution reaction? *Science Bulletin* **62**, 971-973, (2017).

15 Wang, S. *et al.* Arsenopyrite weathering in acidic water: Humic acid affection and arsenic transformation. *Water Research* **194**, 116917 (2021).

16 Kajana, T. *et al.* Potential transition and post-transition metal sulfides as efficient electrodes for energy storage applications. **12**, 18041-18062 (2022).

17 He, R., Huang, X. & Feng, L. Recent Progress in Transition-Metal Sulfide Catalyst Regulation for Improved Oxygen Evolution Reaction. *Energy & Fuels* **36**, 6675-6694, doi:10.1021/acs.energyfuels.2c01429 (2022).

18 Noor, T., Yaqoob, L. & Iqbal, N. J. C. Recent advances in electrocatalysis of oxygen evolution reaction using noble-metal, transition-metal, and carbon-based materials. **8**, 447-483 (2021).

19 Wang, M., Zhang, L., He, Y. & Zhu, H. J. J. o. M. C. A. Recent advances in transition-metal-sulfide-based bifunctional electrocatalysts for overall water splitting. **9**, 5320-5363 (2021).

20 Jin, H. *et al.* Nanocatalyst design for long - term operation of proton/anion exchange membrane water electrolysis. *Adv. Energy Mater.* **11**, 2003188 (2021).

21 He, W. *et al.* Al-doped nickel sulfide nanosheet arrays as highly efficient bifunctional electrocatalysts for overall water splitting. **12**, 24244-24250 (2020).

22 Joshi, P., Riley, P., Goud, K. Y., Mishra, R. K. & Narayan, R. J. C. O. i. E. Recent advances of boron-doped diamond electrochemical sensors toward environmental applications. **32**, 100920 (2022).

23 de Souza, A. B. *et al.* Occurrence and elimination of pharmaceutical residues in municipal wastewater effluent by electrochemical anodic oxidation. **66**, 105899 (2024).

24 Mackuľak, T. *et al.* Boron doped diamond electrode–The elimination of psychoactive drugs and resistant bacteria from wastewater. **171**, 108957 (2020).

25 ZHENG, Y., ZHANG, Y. & TONG, Y. J. J. o. S. C. Research progress and application of boron-doped diamond film. **50**, 1138-1148 (2021).

26 Zhou, Y. L., Tian, R. H., Zhi, J. F. J. B. & Bioelectronics. Amperometric biosensor based on tyrosinase immobilized on a boron-doped diamond electrode. **22**, 822-828 (2007).

27 Zhou, Y. & Zhi, J. J. E. c. Development of an amperometric biosensor based on covalent immobilization of tyrosinase on a boron-doped diamond electrode. **8**, 1811-1816 (2006).

28 Hao, Z., Yuxin, Z., Jun, C. & Yuansheng, P. J. C. J. o. E. E. Direct electrochemical detection of ammonia in wastewater using boron-doped diamond (BDD) electrode. **15**, 4067-4076 (2021).

29 Beka, L. G., Li, X. & Liu, W. Nickel Cobalt Sulfide core/shell structure on 3D Graphene for supercapacitor application. *Scientific Reports* **7**, 2105 (2017).

30 Cheng, J.-W. *et al.* Rational design of nickel cobalt sulfide/cobalt sulfide sheet-on-sheet structure for asymmetric supercapacitors. *Electrochimica Acta* **283**, 1245-1252 (2018).

31 Mohamed Saleem, M. S., Swaminathan, R., Mohan, V., Liyakath Ali, N. U. H. & Kim, S.-J. Sulfurization of cobalt oxide to cobalt sulfide: A positrode for the high-performance supercapacitor. *Journal of Industrial and Engineering Chemistry* **136**, 493-500 (2024).